

## Bundle Formation of Polymers with an Atomic Force Microscope in Contact Mode: A Friction Versus Peeling Process

Z. Elkaakour,<sup>1</sup> J. P. Aimé,<sup>1,\*</sup> T. Bouhacina,<sup>1</sup> C. Odin,<sup>1</sup> and T. Masuda<sup>1,2</sup>

<sup>1</sup>L.C.P.C. Université Bordeaux I, 351 Cours de la Libération 33405 Talence Cedex. France

<sup>2</sup>Department of Polymer Chemistry, Kyoto University, Kyoto 606-01, Japan

(Received 8 June 1994)

Among near field microscopes, the atomic force microscope appears as a powerful and versatile tool for investigating local mechanical properties. In addition, we can take advantage of the tip sample interaction, to perturb, and in turn modify the surface of soft samples. Here we report an attempt to modify the structure of a substituted polyacetylene film spread on a surface. Regular periodic patterns are obtained, and we show that scan frequency and applied load are the pertinent parameters that control the period. These results can be described as bundle formation via a peeling process.

PACS numbers: 61.16.Ch, 06.60.Sx, 81.40.Pq, 83.10.-y

Atomic force microscopy (AFM) in contact mode has opened a wide range of investigation: adhesive properties, tribology, and rheology at submicromic scale. Because of the contact mode, it turns out that the elastic properties of the sample become of primary importance. Particularly for soft samples, this leads to images that involve surface roughness and elastic response of the sample, thus also imaging the mechanical properties [1]. Moreover, for soft materials, one may expect to modify, then to "manipulate," objects and surfaces at the nanometer or submicromic scale. A year ago, it was shown that polystyrene films with a smooth surface exhibit bundles when the tip cantilever in contact mode scratches the surface [2]. Among polymers, conjugated polymers possess specific properties related to the  $\pi$ -electron delocalization along the backbone. They are conducting polymers when they are doped, while numerous applications [3,4] are expected, owing to their optical activity over a large range of wavelengths. A key point is the control of the polymer structure [5]. Here, we have attempted to modify the structure at the chain length scale (a few hundred nanometers) in the hopes that the conjugated backbone properties will be strongly improved. To do this, a first step is to investigate the physical origin of the bundle formation in order to be able to produce well defined ordered and regular patterns.

A soluble polyacetylene of formula  $\{\text{CH}=\text{C}[\text{C}_6\text{H}_4\text{-}o\text{-Si}(\text{CH}_3)_3]\}_n$  was chosen. The molecular weight  $M_w = 230\,000$ , giving a contour length  $L_w = 330\text{ nm}$ . The Young's modulus  $E$  is 700 MPa and the Poisson ratio  $\nu \sim 0.5$  [6]. The glass transition is about 200 °C. A drop of a polymer solution in toluene at a concentration  $c = 3 \times 10^{-2}\text{ g cm}^{-3}$  is deposited either on a mica surface or a lamellar structure ( $\text{WSe}_2$ ), then the solvent gently evaporates. Through a weighing measurement, the thickness of the film is estimated to be 14  $\mu\text{m}$ . The head of the Nanoscope III is inside a glove box under argon atmosphere such that oxygen and water levels in the ppm range are achieved. This avoids capillarity phenomena

and change of the surface tension due to humidity, thus providing well defined, stable, experimental conditions.

A typical, reproducible, pattern is shown in Fig. 1. Because of the friction process, the question arises of material displacement versus stick slip or any kind of sliding effect that may produce change of the cantilever deflection without involving a true roughness. If a true height cannot easily be related to the cantilever deflection, evidence of polymer dragging is shown in Fig. 2. To understand such a picture we shall roughly define two modes: one corresponding to the writing process, the second to the reading process. In both cases, contact mode is used and the reading mode differs from the writing mode only by modification of a few parameters: (i) the frequency at which the scan is performed, (ii) the applied load used, and (iii) the sweeping number before the image is recorded. In other words, the reading versus writing case is simply obtained by minimizing the perturbing experimental conditions.

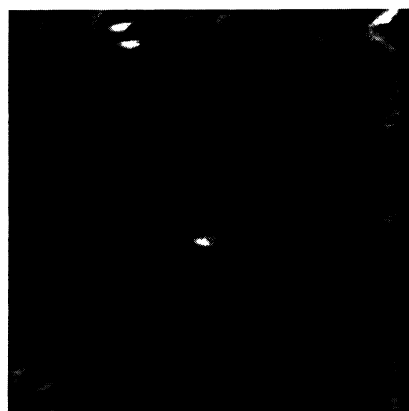


FIG. 1. AFM image showing the typical structure obtained. This image has been recorded after one scan (tip velocity  $10\ \mu\text{m s}^{-1}$ ) on a region  $1\ \mu\text{m}$  by  $1\ \mu\text{m}$ . All the experiments were performed with a Nanoprobe cantilever for which the estimate stiffness is  $0.6\ \text{N m}^{-1}$ .



FIG. 2. 256 scans were performed at fixed  $Y$  position (disabled mode) for four different orientations (tip velocity  $80 \mu\text{m s}^{-1}$  and applied load 100 nN), then an image was "read" in  $XY$  mode with the same velocity and applied load of 50 nN and in one scan. The scan size is  $4 \mu\text{m}$  by  $4 \mu\text{m}$ .

In order to set as accurately as possible the pertinent physical parameters, experiments were performed at a fixed  $Y$  position. The main reason is the following: Because of a finite size of the cantilever tip, the area of the contact between the tip and the polymer surface induces a perturbation length. An order of the magnitude of this length can be obtained by using the Johnson-Kendall-Roberts model [7] that includes the adhesion force in the Hertz theory. For example, for a hemispheric tip apex with a radius  $R$  of 40 nm, a load equal to 100 nN gives a contact area radius  $b$  of about 15 nm and an indentation depth  $h$  equal to 3 nm. Thus, the perturbation length given by the cantilever tip is about  $\frac{1}{20}$  of the polymer length in its extended conformation. On the other hand, when the experiment is performed with an  $X$ - $Y$  scan at row  $J + 1$ , the tip is modifying a polymer film already perturbed at the row  $J$ . Therefore, the ratio of the scan resolution length  $\Delta Y_{J,J+1}$  versus the size of the contact area is a parameter that may modify the quality of the chain alignment.

Most of the experiments were thus performed at a fixed  $Y$  position, creating a wrinkle along the  $X$  line. So, the  $Y$  coordinates give the sweeping number in Figs. 3, 4 and 5. Structures obtained for the same scan size at different scan frequencies are shown in Fig. 3. Scans were also performed at a larger scale in order to check the larger tip velocity as well as the influence of the scan size [Figs. 4(a)–4(b)]. In both cases, a frequency dependence is observed. At low velocity, the length between bundles shows a monotonic decrease as the tip velocity increases (Fig. 6). At larger probe tip velocities, typically above  $10 \mu\text{m s}^{-1}$ , we were unable to measure any meaningful variations of the period. A plateaulike behavior is observed in that velocity range, which is interpretable as a direct result of a lack of sensitivity to small relative changes.

Other important parameters should be the contact area and penetration depth of the tip in the polymer film,

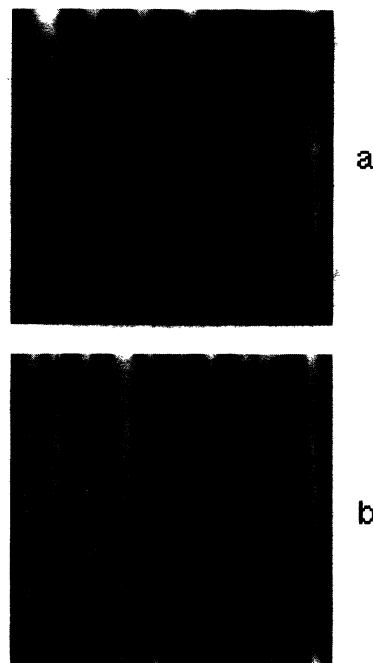


FIG. 3. Scan obtained at fixed  $Y$  position. The image size is  $1 \mu\text{m}$  with tip velocity (a)  $0.1 \mu\text{m s}^{-1}$  and (b)  $30 \mu\text{m s}^{-1}$ . The maximum  $Y$  coordinate corresponds to 256 scans at a given  $Y$  position in the  $XY$  plan.

the two being governed by the magnitude of the applied load. Figure 5 shows the structure at two different loads. The distance between bundles increases as the applied load increases (Fig. 7). Any attempt at recording the height changes of the bundles as a function of the

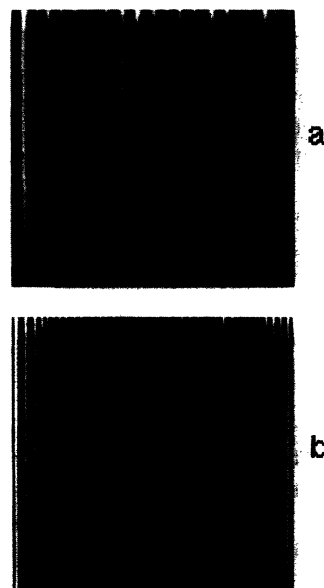


FIG. 4. Images obtained after scanning with the disabled mode (fixed  $Y$  position) (a):  $X$  size  $2 \mu\text{m}$  (tip velocity  $20 \mu\text{m s}^{-1}$ ) and (b):  $X$  size  $4 \mu\text{m}$  (tip velocity  $80 \mu\text{m s}^{-1}$ ). The images reported here correspond to a second measurement for which the scan number is varying between 256 and 512.

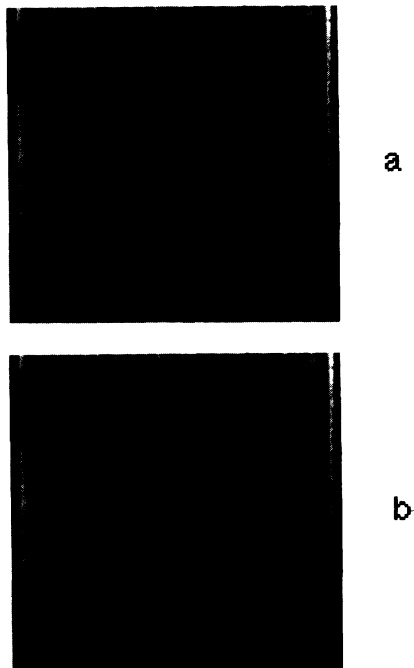


FIG. 5. Scan obtained at fixed  $Y$  position for two different loads. The image size is  $2 \mu\text{m}$  (tip velocity  $20 \mu\text{m s}^{-1}$ ), (a)  $100 \text{ nN}$ , (b)  $150 \text{ nN}$ . The maximum  $Y$  coordinate corresponds to 256 scans at a given  $Y$  position in the  $XY$  plan.

frequency, load, or sweeping number is quite difficult. This is because the elastic properties of the bundles can change, owing to variations of the local density and chain arrangement inside the bundle. Such changes do not allow us to compare the height deflections measured at different stages or under different conditions since they do not always probe the same properties. Nevertheless, one can estimate a maximum height after a hundred scans

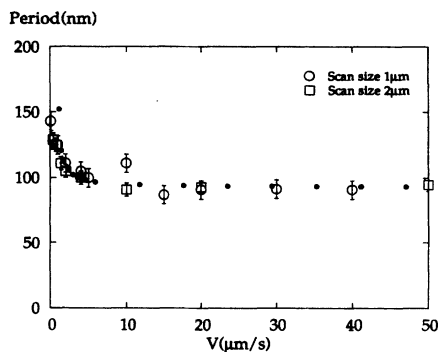


FIG. 6. Variation of the distance between bundles versus the probe tip velocity for two scan sizes. A monotonous decrease is observed up to  $10 \mu\text{m s}^{-1}$ , then a plateau. The experiments were performed at the load  $100 \text{ nN}$ . The periods were measured after 200 scans. Black circles are theoretical computations. The theoretical computation is similar to the one used in Ref. [8]. Constants used are  $W_0 = 50 \text{ mJ m}^{-2}$ ,  $\alpha = 6500 \text{ (MKSA)}$ , and the exponent  $n = 0.6$ .

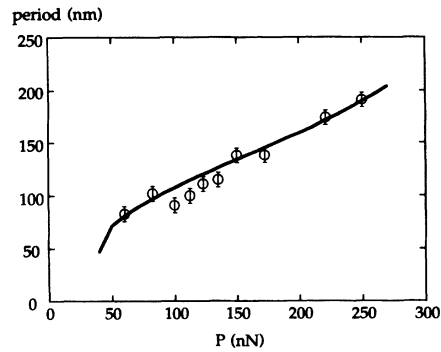


FIG. 7. Variation of the distance between bundles versus the load for a tip velocity  $10 \mu\text{m s}^{-1}$ . The periods were measured after 200 scans. The line corresponds to the theoretical computation.

that ranges from  $40$  to  $70 \text{ nm}$ . We thus have to take into account the velocity and load effects together with the material displacement. In order to describe the whole process, we consider a fracture mechanism in which energy dissipation occurs at the crack tip.

We shall consider a process similar to the peeling one, in which a strip of polymer is pushed ahead the cantilever tip. The lateral probe tip motion yields a strain  $\Delta$ , producing a stress inside the polymer film. The release of that constraint is achieved through the propagation of a crack. This crack propagation is controlled by an energy balance reminiscent of Griffith's criterion [8]. Let's note the surface energy term  $W$  that controls the crack opening and the strain energy release rate  $G$  which is given by [9]

$$G = E \frac{h}{2} \left( \frac{\Delta}{L} \right)^2, \quad (1)$$

where the different parameters involved are given in Fig. 8. Thermodynamic equilibrium is obtained by equating  $G$  to  $W$ . The velocity dependence of the period can be understood through the introduction of viscoelastic loss at the crack tip. A general expression has been given by the WLF model [10], from which an explicit dependence of

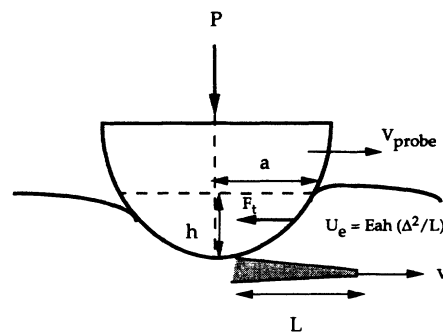


FIG. 8. Sketch of the tip-sample contact and crack opening.  $U_e$  is the elastic energy stored into the polymer sample under the lateral cantilever tip motion  $\Delta$ . The crack tip velocity is given by  $G = W$  and  $V_{\text{probe}} = d\Delta/dt$ .

the crack tip velocity is given. The surface energy term becomes

$$W = W_0(1 + \alpha v^n), \quad (2)$$

where  $\alpha$  is a material constant and  $v = dL/dt$  the crack tip velocity, and  $n$  is an exponent which is found to be equal to 0.6 for the polyurethane, but may have other values depending on the polymer used [8].

The elastic energy stored in the polymer induces a tangential force that applies on the tip apex (Fig. 8) and is given by [9]

$$F_t = \frac{Eah}{2} \frac{\Delta}{L}. \quad (3)$$

Note that Eqs. (1) and (2) correspond to a peeling process for which the probe stiffness is much larger than the sample stiffness (which is a correct approximation for the tangential force) and that the peeling corresponds to a mode I failure.

Following Mindlin [11], we define a critical force above which the tip slip on the surface. When the adhesive force is taken into account, the tangential force leading to the sliding motion is a function of the adhesive force and the vertical applied load [12–15]. Here, we shall consider the relation given in Refs. [14] and [15]:

$$F_t^s = \mu P_1, \quad (4)$$

where  $\mu$  is the coefficient of friction and  $P_1$  the equivalent load taking into account the increase of the contact area due to the work of adhesion [7]:

$$P_1 = P + 3\pi RW + \sqrt{6\pi RWP + (3\pi RW)^2}, \quad (5)$$

where  $P$  is the vertical applied load. As soon as  $F_t$  reaches the critical value  $F_t^s$ , the probe tip no longer peels the sample and slides above the polymer accumulated in the bundle. Theoretical results are reported in Figs. 6 and 7. Such an approach provides useful understanding of the bundle formation but is obviously crude. Our experimental situation differs from the above model in several ways.

(i) We do not have access at any relation between the geometry of the crack tip and the geometry of the contact area between the probe tip and the polymer, therefore to changes on the crack geometry as a function of the load.

(ii) The above model works as a hit-or-miss process, avoiding the fact that the increase of the tangential force during the peeling decreases the contact area [11,12], therefore modifying the efficiency of the process. The latter should lead to a transition between the crack propagation (the peeling) and the sliding motion of the cantilever tip smoother than the one suggested in the above.

The main interest of this model is to reproduce the main features reasonably well, thus providing an understanding of the general behavior observed as a function of the frequency and load. From the present results, predictions can be made that allow us to produce a given pattern as a function of the tip geometry, load, and frequency. For conjugated polymers it remains to be seen how far their properties are improved. The knowledge of the chain-chain interactions, and of the chain conformation are of prime importance for understanding the transport and spectroscopic properties. Also, it remains that the patterns produced up to now are at most at 5  $\mu\text{m}$  scale. Therefore, a near-field microscope with an optical fiber with a radius of curvature on the nanometer scale would be needed to investigate the yield of luminescence, allowing comparison of the properties of the amorphous part and of the bundle structure.

This work was supported in part by Conseil Régional d'Aquitaine.

---

\*To whom correspondence should be addressed.

- [1] M. Radmacher, R. W. Tillman, M. Fritz, and H. E. Gaub, *Science* **257**, 1900–1905 (1992).
- [2] On Man Leung and M. Cynthia Goh, *Science* **255**, 64–66 (1992).
- [3] N. C. Greenham, S. C. Moratti, D. D. C. Bradley, R. H. Friend, and A. B. Holmes, *Nature (London)* **365**, 628–630 (1993).
- [4] See, for example, the review in *Conjugated Polymers*, edited by J. L. Brédas and R. Silbey (Kluwer, Dordrecht, 1991), p. 555.
- [5] T. Schimmel, D. Gläser, M. Schwoerer, and H. Naarman, *Ref. [4]*, p. 49.
- [6] T. Masuda, T. Hamano, K. Tsuchihara, and T. Higashimura, *Macromolecules* **23**, 1374 (1990).
- [7] K. L. Johnson, K. Kendal, and A. D. Roberts, *Proc. R. Soc. London Sect. A* **324**, 301 (1971).
- [8] D. Maugis, *J. Mater. Sci.* **20**, 3041–3073 (1985).
- [9] M. Barquins, *J. Appl. Polym. Sci.* **29**, 3269–3282 (1984).
- [10] J. D. Ferry, *Viscoelastic Properties of Polymers* (Wiley, New York, 1970), p. 292.
- [11] R. D. Mindlin, *J. Appl. Mech.* **16**, 259 (1949).
- [12] A. R. Savkoor and G. A. D. Briggs, *Proc. R. Soc. London Sect. A* **356**, 103–104 (1977).
- [13] C. Thornton, *J. Phys. D. Appl. Phys.* **24**, 1942–1946 (1991).
- [14] K. Kendall, *Nature (London)* **319**, 203–205 (1986).
- [15] M. Barquins, in *Wear and Friction of Elastomer*, edited by R. Denton and M. K. Keshavan (American Society for Testing Materials, Philadelphia, 1992).

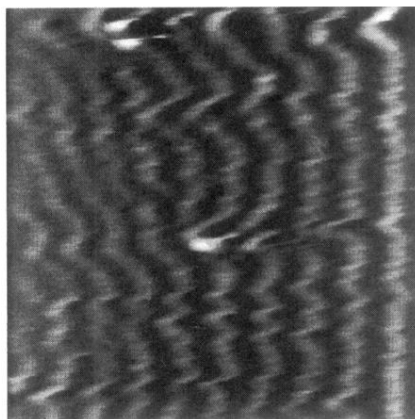


FIG. 1. AFM image showing the typical structure obtained. This image has been recorded after one scan (tip velocity  $10 \mu\text{m s}^{-1}$ ) on a region  $1 \mu\text{m}$  by  $1 \mu\text{m}$ . All the experiments were performed with a Nanoprobe cantilever for which the estimate stiffness is  $0.6 \text{ N m}^{-1}$ .

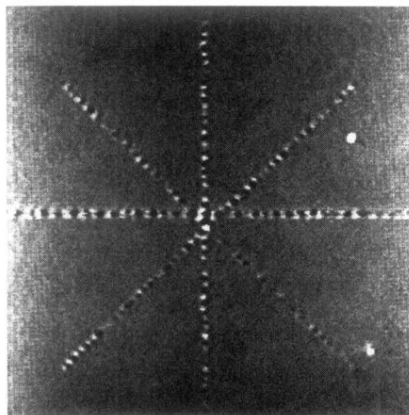


FIG. 2. 256 scans were performed at fixed  $Y$  position (disabled mode) for four different orientations (tip velocity  $80 \mu\text{m s}^{-1}$  and applied load 100 nN), then an image was "read" in  $XY$  mode with the same velocity and applied load of 50 nN and in one scan. The scan size is  $4 \mu\text{m}$  by  $4 \mu\text{m}$ .

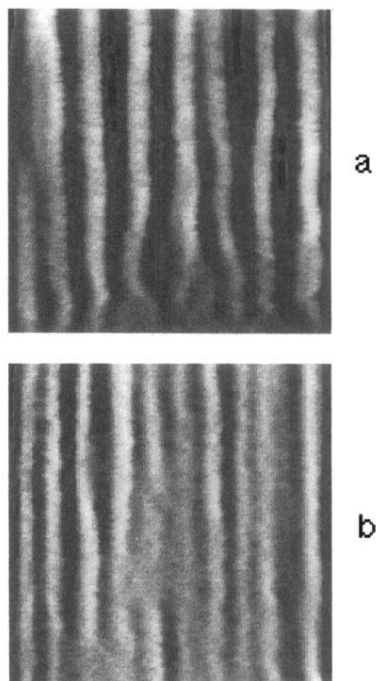


FIG. 3. Scan obtained at fixed  $Y$  position. The image size is  $1 \mu\text{m}$  with tip velocity (a)  $0.1 \mu\text{m s}^{-1}$  and (b)  $30 \mu\text{m s}^{-1}$ . The maximum  $Y$  coordinate corresponds to 256 scans at a given  $Y$  position in the  $XY$  plan.

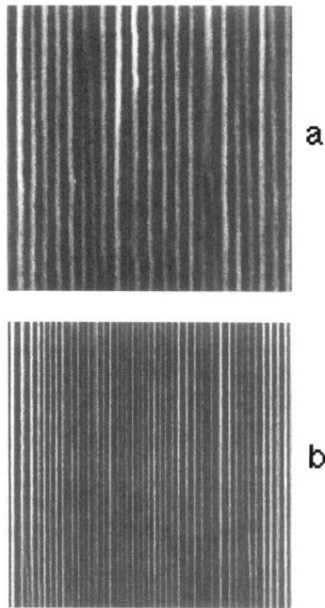


FIG. 4. Images obtained after scanning with the disable mode (fixed  $Y$  position) (a):  $X$  size  $2 \mu\text{m}$  (tip velocity  $20 \mu\text{m s}^{-1}$ ) and (b):  $X$  size  $4 \mu\text{m}$  (tip velocity  $80 \mu\text{m s}^{-1}$ ). The images reported here correspond to a second measurement for which the scan number is varying between 256 and 512.



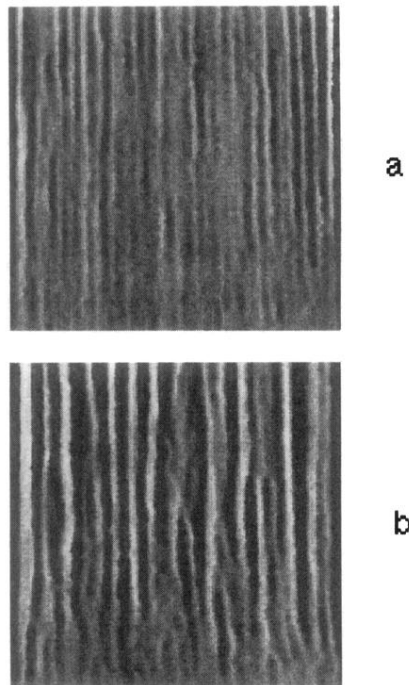


FIG. 5. Scan obtained at fixed  $Y$  position for two different loads. The image size is  $2\ \mu\text{m}$  (tip velocity  $20\ \mu\text{m s}^{-1}$ ), (a) 100 nN, (b) 150 nN. The maximum  $Y$  coordinate corresponds to 256 scans at a given  $Y$  position in the  $XY$  plan.

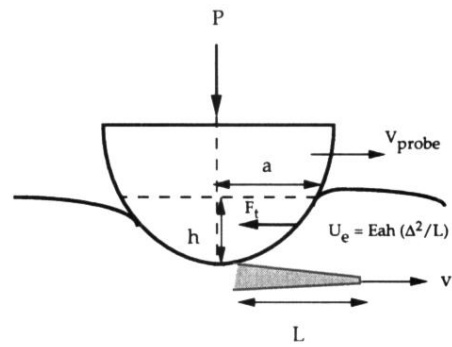


FIG. 8. Sketch of the tip-sample contact and crack opening.  $U_e$  is the elastic energy stored into the polymer sample under the lateral cantilever tip motion  $\Delta$ . The crack tip velocity is given by  $G = W$  and  $V_{\text{probe}} = d\Delta/dt$ .